Jül-Conf-45 B6

I C A N S - V
MEETING OF THE INTERNATIONAL COLLABORATION ON
ADVANCED NEUTRON SOURCES
June 22-26, 1981

# High Energy Particle Spectra from Spallation Targets

S. Cierjacks, F. Raupp, S.D.Howe, Y. Hino, M.T. Swinhoe,
M.T. Rainbow and L. Buth

Kernforschungszentrum Karlsruhe
Institut für Kernphysik
7500 Karlsruhe, Postfach 3640
Federal Republic of Germany

Abstract:
The experimental program of high energy spectra measurements performed in conjunction with the feasibility study for a German spallation source is surveyed. This program included the measurement of angular and depth dependent neutron and charged-particle yields and spectra from thick targets, the determination of high energy neutron spectra associated with moderated beams and the measurements of neutron and charged-particle production cross sections from various thin targets by 590 and 1100 MeV protons. Since absolute measurements of neutron data depend on the accurate knowledge of the neutron detection efficiency of scintillation counters, auxiliary measurements of this quantity were performed in the neutron region 50 to 450 MeV.

## 1. INTRODUCTION

High energy particle spectra from spallation targets by 590 and 1100 MeV protons were measured as part of the project study for a German spallation neutron source. In this context depth and angular dependent yields and spectra of neutrons and charged-particles leaking out from thick bare metal targets were of primary interest. The accurate knowledge of these quantities is an important prerequisite for a realistic estimate of the specifications of a spallation source, because the bare target data determine all

subsequent particle transport in the moderator and the reflector of a particular target assembly.

In parallel to the study of yields and spectra from the bare target also the spectra of the fast neutrons were measured which are scattered in the moderator and which are emitted together with the thermal neutrons through the beam holes of a shielded target assembly. Since for this type of measurements the time-of-flight method was not applicable, a new technique was employed which is based on spectrum unfolding of analog data. A large fraction of fast neutrons in a moderated neutron beam may cause shielding problems and can cause additional undesirable background in some experiments with thermal and epithermal neutrons.

Beginning of this year additional experiments were started to measure neutron and charged-particle production cross sections from thin spallation targets covering a wide range of masses from carbon to uranium. The measurements of differential production cross sections aimes at a better understanding of the spallation process and can be used to test the nuclear models underlying the existing high-energy transport codes such as the High-Energy Nucleon-Meson Transport Code, HETC (1).
A final auxiliary program concerned the experimental determination of neutron detection efficiencies at high energies. While reliable data are well established below $\sim$ 70 MeV from various experiments and calculations, detection efficiencies above that energy rely almost completely on Monte Carlo calculations for this quantity.

## 2. HIGH ENERGY PARTICLE YIELDS AND SPECTRA FROM THICK TARGETS

### 2.1 Experimental Details

The measurements were performed at the SIN cyclotron providing 590 MeV protons and at the LNS synchrotron providing 1100 MeV protons. A schematic view of the target-detector arrangement as used for the SIN experiments is shown in Fig. 1. The proton beam was focussed to 2 cm diameter onto the cylindrical lead target. This was composed of twelve cylindrical blocks, each 5 cm long and 10 cm in diameter, to give an overall length of 60 cm. Time-of-flight

measurements of the neutrons produced were made using the cyclotron microstructure pulsing at 16.9 MHz repetition rate and of $< 0.2$ ns pulse width.

Neutrons emitted from the target at $30^{\circ}$, $90^{\circ}$ and $150^{\circ}$ were detected at the exit of a $\sim$ 1 m long iron collimator. Depth dependent measurements of neutron spectra were made by moving the target along the beam axis, so that the individual blocks were opposite the collimator entrance. The principal detector was a 3 cm thick, 4,5 cm diameter, NE 213 liquid scintillator employing n-$\gamma$ pulse-shape discrimination (PSD). In order to remove pulses from charged particles also produced in the target, a 5 mm thick plastic scintillator placed in front of the principal detector was used as a veto counter. (While neutron and $\gamma$-rays produce in general a signal in only one of the detectors, charged particles from the target are characterized by signals in both counters).

Background measurements at $90^{\circ}$ were performed with the target block opposite the collimator entrance removed. For $30^{\circ}$ and $150^{\circ}$ shaped wedges were used to give the relevant background contribution.

The experimental arrangement at SATURNE was similar to that shown in Fig.1. But, due to the lower pulse repetition rate of 7.3 MHz for the SATURNE machine a longer flight path of 3 m was employed. In this case an auxiliary iron collimator, 0.5 m thick, was placed in front of the neutron detector.

Data accumulation was accomplished in a 4-parameter mode. A block diagram of the electronics is shown in Fig. 2: The pulse-height signal from the liquid scintillator was split into two amplifier channels, one with ten times the gain of the other. This was necessary to cover the large total dynamic range and the expanded threshold region (an accurate measurement of the effective detector threshold is an important prerequisite for a precise detector efficiency determination). The timing signal of the neutron detector served three functions:

1. It started the main TAC which provided the neutron time-of-flight via ADC 4. This TAC was stopped by a timing signal derived from the cyclotron r.f.
2. It provided the input signals for the n-$\gamma$ pulse-shape discrimination circuit providing an identification signal which went to ADC 3.

3. It was used in conjunction with the fast signal from the veto detector to generate a master trigger signal which notified the computer that a neutron or a γ-event occured and that the gates to the ADCs should be opened.

The contents of the four ADCs were stored event-by-event on magnetic tape for subsequent off-line data processing. The number of master triggers applied to the computer was recorded and used in conjunction with the number of accepted events to evaluate dead-time effects.

At the SIN the proton current was measured throughout the experiment by a proton beam monitor (see Fig. 1). This monitor consisted of a carbon scatterer placed in the incident proton beam. Scattered protons were detected by a pair of thin plastic scintillators which operated in coincidence. The monitor was calibrated with respect to absolute proton flux by counting individual protons in the direct beam with a third thin plastic scintillator at sufficiently reduced current. The proton-current measurement at SATURNE was accomplished by three different detector systems:
1. A proton telescope counter similar to that used at SIN,
2. an ionization chamber and
3. a secondary electron emission chamber.
All three systems were calibrated simultanously by carbon activation employing the well known $^{12}C\ (p,x)^{11}C$ activation cross section.

## 2.2 Off-Line Data Processing

The analysis of neutron yields and spectra began with the separation of neutron and γ events by a consideration of 2-dimensional arrays of pulse height versus "pulse shape discrimination time". Excluding γ-events from further analysis the neutron events from the corresponding background runs were then substracted. These data were subsequently sorted into suitable time-of-flight bins and their corresponding energies calculated relativistically according to the time of occurence of the prompt γ- peak.
In typical time-of-flight measurements a single overlap in part of the neutron time-of-flight spectrum was admitted. Seperation of the response due to high energy neutrons from that due to low energy neutrons was

achieved by linear extrapolation of the high energy pulse height response down to the bias level. The error associated with this procedure is small because of the largely different shapes of the corresponding distributions.

The contents of each time bin were integrated and the results divided by the detection efficiency of the NE 213 neutron detector. The Monte Carlo Code of Stanton as modified by Cecil et. al. (2) was used to calculate the required efficiency. The shape of the pulse height spectra produced by the code were in good agreement with the measured spectra in the various time bins. This was the case even when the ranges of charged particles produced in the detector are greater than the detector dimensions. This fact in conjunction with experimental tests of the original code in various laboratories up to 70 MeV (3) and with own measurements between 50 and 450 MeV (compare section 5) gives confidence in the operation of the code.

The data were finally scaled by the solid angle subtended by the detector, the energy bin width, the dead time correction factor and the number of incident protons to produce the absolute neutron yields as neutrons per proton, per steradian, per MeV and per $cm^2$ target surface. Finally the results for various distances into the target were added to produce the absolute angular dependent neutron yield from the whole target. The measured neutron spectra were corrected for the measured time resolution of the system using the second derivative method (4).

## 2.3 Results

Fig. 3 shows a typical spectrum measurement obtained for lead with 590 MeV protons. This result represents the sum of the $90^{\circ}$ depth-dependent spectra for the whole target length. This spectrum exhibits the well known two-component shape originating from contributions of evaporation processes and direct cascade reactions (the latter of which produces the broad shoulder around 50 MeV). In Fig. 3 the measured $90^{\circ}$ spectrum is compared to a recent calculation performed at KFA Jülich (5). The calculational method is based on the 3-dimensional "High Energy Nucleon-Meson Transport Code, HETC" (1). As can be seen from this comparison the calculations produce at the present time much softer spectra than observed in the measurements.

Three depth dependant neutron spectra obtained from a thick uranium target by 590 MeV protons are shown in Fig. 4 (6). They correspond to the neutron yields obtained at $90^{o}$ to the incident proton beam and 2.5, 7.5 and 12.5 cm depths into the target. The upper curve and the two lower curves were measured in two different runs at the SIN involving different pulse repetition rates. Therefore, the detector threshold was set to a much higher value in the two bottom curves than in the top curve. It can be seen from the upper yield curve that the uranium spectrum is significantly softer than the respective lead spectrum (comp. Fig. 3). This together with the by a factor of two higher n/p value provides an additional advantage, when uranium is used as the primary target for a moderated source, because a larger fraction of the total neutron spectrum is moderated.

The spectral distribution of neutrons emitted at $90^{o}$ from a 2.5 cm average target depths of a thick lead target is shown in Fig. 5 for 590 MeV and 1100 MeV proton energy. Except for the higher energy limit of the spectrum and the by a factor of 1.3 higher n/p value for 1100 MeV proton energy both spectra are very similar.

The difference for incident proton energies of 590 MeV and 1100 MeV is more pronounced for the spectra of secondary protons emitted at $90^{o}$ from thick lead targets as shown in Fig. 6. These data were also taken for an average target depth of $2.5 \pm 2$ cm. The high fraction of high energy protons, particularly for 1100 MeV incident beam energy may have some implications for the installation of a cold neutron source. Thus it could be worthwhile for the sake of a lower heat deposition to choose a larger diameter for the primary target.

## 3. MEASUREMENTS OF THE HIGH ENERGY COMPONENT OF THE NEUTRON SPECTRUM FROM A MODERATED SOURCE

The neutron spectrum from a moderated source covers the energy range from thermal to hundreds of MeV. The range of interest for these measurements of the "high energy" part of the spectrum includes all those neutrons above a few MeV. Even though time-of-flight measurements of fast neutron spectra would have been most desirable, this method was not applicable at the SIN

cyclotron and the SATURNE accelerator where the only useful pulse comes from the machine microstructure. This time structure is much too narrow compared with the large time spread associated with the moderation process and so an unfolding method was necessary.

The moderated source studied at the SIN was a 15 cm diameter heavy metal target (lead or uranium) in a cubic tank ( of side 2 m ) of light water. The detector, an 8.9 cm thick NE 213 scintillator, was placed approximately 8 m from the target at $30^{o}$ to the incident beam direction. The collimator defined a region above the bare target so that neutrons coming directly from the target could not be seen. The same electronics and data recording system were used as for bare target measurements described above, with the omission of the time-of-flight parameter. The general target configuration used at Saturne is shown in Fig. 7. The primary target was a large 50 by 50 cm, 10 cm high, heavy metal block (lead or uranium). The centre part which was directly hit by the proton beam was composed of alternately arranged plates of metal, polyethelene and aluminum, in order to simulate a realistic spallation neutron target design. The polyethylene and the aluminum represented the coolant and the structural material. A polyethylene moderator was placed on top of the primary target and surrounded by a 20 cm thick reflector (lead or beryllium).

The results obtained for the four described target configurations are shown in Fig. 8. These were obtained by rectangularly unfolding the pulse height distributions of the detector and are normalized to 5 mA and 10 mA, for 1100 MeV and 590 MeV protons respectively, at a distance of 6 m from the target. It can be seen that the distributions are very similar for lead and uranium targets. The sharp cut-off of the spectra above about 100 MeV is mainly due to a combined effect of the small detector size and the adopted simplified unfolding method. With respect to the detector only a commercial 8.9 cm long liquid scintillator was available during the early phase of the program. In such a detector very high energy particles are not completely stopped. The simplified method of rectangular unfolding was applied mainly because it allowed a quick data analysis while providing a rather good estimate of the total number of fast neutrons and the spectrum below ~100 MeV as verified by computer simulations of the experiments (7 ).

The disadvantage of the described unfolding method which underestimates the fraction of high energy neutrons was avoided in a recent experiment which employed a self-built, 30 cm long, liquid scintillator and an iterative method of spectrum unfolding (8). In this experiment the earlier measurement on the lead-polyethelene-lead target configuration was repeated. A comparison of the results obtained with the two methods is shown in Fig. 9. In order to enhance the differences in the two methods only the smoothed lines drawn through the original data points are shown in this diagram. It can be seen that both unfolding methods give the same spectrum below about 50 MeV and approximately the same integral number of neutrons. However, the spectrum above 50 MeV is increasingly distorted with increasing energy when the previous unfolding method is applied.

## 4. PARTICLE PRODUCTION CROSS SECTION MEASUREMENTS

### 4.1 Neutron Production Cross Sections

Neutron production cross sections of C, Al, Fe, In, Ta, Pb and U by 590 MeV were measured at the SIN at angles of $30^{o}$, $90^{o}$ and $150^{o}$. In this case the same collimator arrangement as shown in Fig. 1 was used. Thin metal plates of 10x10 cm, a few mm thick, were used as neutron targets. The proton beam was focussed to 1 cm onto the centre of the target. Data aquisition and data analysis was analogous to that involved for the thick sample measurements. A first result of these measurements is shown in Fig. 10. The measured differential production cross section is compared with a recent HETC calculation performed by Armstrong et al. (9). The measured and calculated absolute cross sections are in excellent agreement below ~20 MeV. In the cascade region the calculations give much lower values than the measurements similar as for the thick target yields. In view of the discrepancies between measured and calculated values it was intresting to compare our results also with previous measurements performed at 800 MeV in Los Alamos (10). Even though both measurements are not directly comparable there is an obvious similarity of the spectrum shapes in the cascade region. The sligthly smaller cross section at the very high energy end of the spectrum may at least be partly explained by the larger observation angle for the Los Alamos experiment.

## 4.2 Charged-Particle Production Cross Sections

Charged-particle production cross sections can be measured with the same apparatus as that used for neutrons. In this case the liquid scintillator is operated in coincidence with the adjoint thin plastic scintillator (comp. Fig. 1). The identification of different charged particles must be accomplished by their specific energy losses in the main detector. This can be done by consideration of the two-dimensional arrays of pulse-height versus particle time-of-flight. The theoretical relationship between energy deposition and particle time-of-flight is shown in Fig. 11. The given relationship applies for a detector of the size used for our experiments. For this detector the range of the particles with the utmost possible energy is much larger than the detector size. Therefore all individual curves peak at those energies where the the particle range in the detector is equal to the detector length. Above the maximum the monotonic decrease with energy is caused by the decreasing specific energy loss over the fixed detector length. It is obvious from Fig. 11 that the difference in the various curves allows good particle separation over most of the total energy range. It is also advantageous that the particle spectra for deuterons, tritons and $\alpha$-particles drop rapidly with energy, so that even the crossing areas for different particles don't cause major problems in the off-line analysis of raw data. Thus only the separation of pions and very high energetic protons remains comparatively problematic. A typical result obtained by the described type of analysis is shown in Fig. 12. This exhibits the relative charged -particle spectra observed from a thin lead target by bombardment with 590 MeV protons. Besides secondary protons also deuterons, tritons, $\alpha$-particles and charged pions were measured. For the sake of clarity the pion spectrum was not included in this diagram. Since the displayed lead data stemmed from an early orientational run no absolute production cross sections were calculated.

Extensive charged-particle production cross section measurements have recently been performed for 590 MeV protons at the SIN. In these experiments an "open geometry" was used. This was possible, because room-scattered background events are severely reduced by the telescope-type of measurement which is strongly directional selective. Due to the high particle threshold caused by the plastic coincidence counter flight paths of up to 4 m could be em-

ployed without causing any time overlap from successive machine pulses. Various charged-particle results which have been obtained from the recent SIN experiment are presented in a workshop contribution of this conference (11).

## 5. MEASUREMENTS OF NEUTRON DETECTION EFFICIENCIES

As stated in section 1 absolute neutron spectrum measurements require an accurate knowledge of the detection efficiency for the employed neutron detectors. For neutron energies below 70 MeV various codes have been established in the past which provide accurate predictions of typically 5 - 10% This was verified by numerous comparisons of code predictions with experimental efficiency determinations ( 3). However, to our knowledge the only measurement up to 225 MeV is that of Mc Donald et al. (12) which shows partly rather poor agreement with Monte Carlo code predictions of Cecil et al.( 2). Therefore, auxiliary measurements were carried out at the SIN to determine the detection efficiency for our neutron detecor in the energy range from 50 MeV to 450 MeV. For this purpose the neutron facility of the Freiburg University group was employed. A schematic diagram of the experimental arrangement used for the efficiency determination is shown in Fig. 13. The primary neutrons were produced by 590 MeV protons incident on a 9 cm thick beryllium target. The neutron spectrum provided by this source at an angle of $3^{o}$ exhibits a pronounced peak between 470 and 570 MeV. Only this part of the neutron spectrum was used for our experiment. A narrow neutron beam was produced by several collimators placed at different positions along the 60 m long flight path. Charged-particles and $\gamma$-rays were removed from the incident neutron beam by cleaning magnets and an 8 cm long $\gamma$-filter in the beam line. The elastic scattering of the neutrons in a liquid hydrogen target was used to determine the detection efficiency by means of the associated particle method. Since the elastic scattering in the hydrogen target produces equal numbers of protons and neutrons, the detector efficiency can be derived by the number of detected neutrons related with the number of protons measured in the kinematically related solid angle. The selection of neutrons in a narrow energy band was accomplished from proton time-of-flight measurements with the two proton detectors. For variation of the neutron detection energy measurements were made at different scattering angles.

The results obtained from our efficiency measurements are shown in Fig. 14. The detection efficiency for the 4.5 cm diameter, 3 cm thick, NE 213 liquid scintillator was determined for three different thresholds of 0.6, 4.2 and 17.5 MeV electron energy ($MeV_{ee}$). The corresponding efficiencies predicted by the Cecil code are in good agreement with the measured values. Only for the 17.5 $MeV_{ee}$ threshold the two data points above 300 MeV are systematically higher than the predictions which could be due to the fact that the code of Cecil does not include pion production.

## 6. CONCLUSION

The experimental program persued during the last two years in conjunction with the project study for a German spallation neutron source has provided a large number of accurate high energy spectra results. These results together with recent neutron production cross section measurements from Los Alamos have revealed some significant inconsistencies with existing theoretical model calculations, particularily in the cascade energy region. It appears,therefore, worthwhile to intensify specific comparisons of experimental results and model calculations. Apart from thick target yields and spectra absolute neutron and charged-particle production cross section measurements provide a useful tool to efficiently test the underlying nuclear models used in existing high energy nucleon-meson transport codes.

The authors acknowledge the help provided during the measurements by the SIN staff,especially Dr. W. Fischer and Dr C.Tschalär, and by the LNS staff, particularily Dr. F.Faure, Dr.G. Milleret and Dr. J. Siret

## REFERENCES

1. HETC - ORNL - 4744 (Oak Ridge National Laboratory)
2. R.A.Cecil, B.D. Anderson and R.Mady, Nucl. Instr. and Meth.161,439(1979)
3. N.R. Stanton, Report, COO-1545-92 (1971)
4. H.W.Schmitt, W.E. Kiker and C.W. Williams, Phys Rev.B137,837(1965)
5. D. Filges,P. Cloth, R.D.Neef,G. Sterzenbach, Contr. to Spallation Source Meeting, Bad Königstein, 18-20 March 1980

6. F. Raupp, S. Cierjacks, Y. Hino, S.D. Howe, M.T. Rainbow, M.T. Swinhoe, L. Buth, contribution to this conference
7. S. Cierjacks, M.T. Rainbow, M.T. Swinhoe, L. Buth, KfK-Report, KfK 3097B, Dec 1980
8. Y. Hino, S. Cierjacks, S.D. Howe, F. Raupp, M.T. Rainbow, M.T. Swinhoe, L. Buth, contribution to this conference
9. T.W. Armstrong, private communication
10. S.D. Howe, PhD Thesis, Kansas State University, 1980
11. S.D. Howe, S. Cierjacks, Y.Hino, F. Raupp, M.T.Rainbow, M.T. Swinhoe, L. Buth, contribution to this conference
12. W.J. Mc Donald, A. Anderson, L. Antonuk, W.K. Dawson, D.A. Hutchson, P.Kitching, C.A. Miller, D.M. Sheppard, Nucl. Instr. Meth. 166,187 (1979)

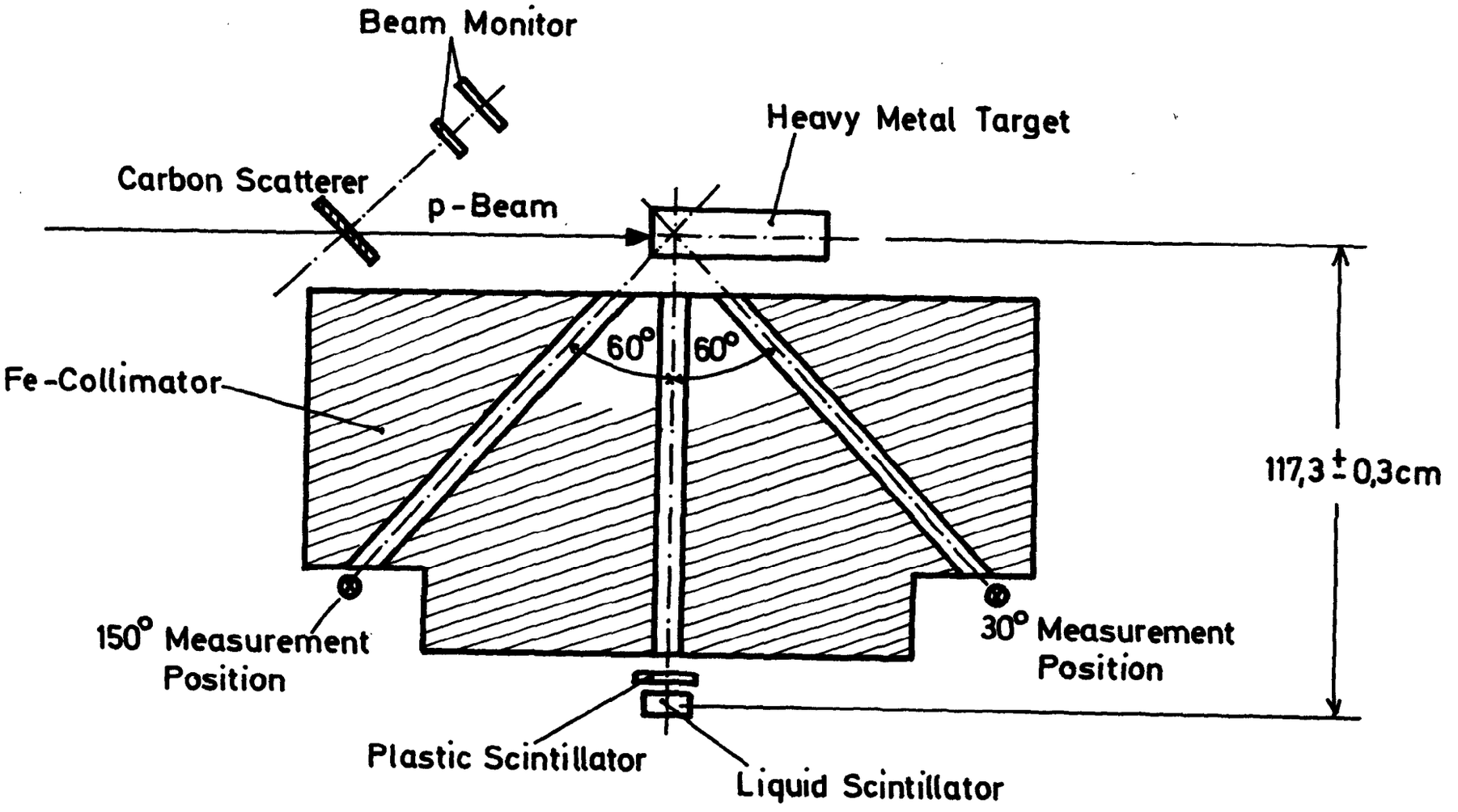


Figure 1 - Schematic diagram of the experimental arrangement used for the SIN time-of-flight experiments

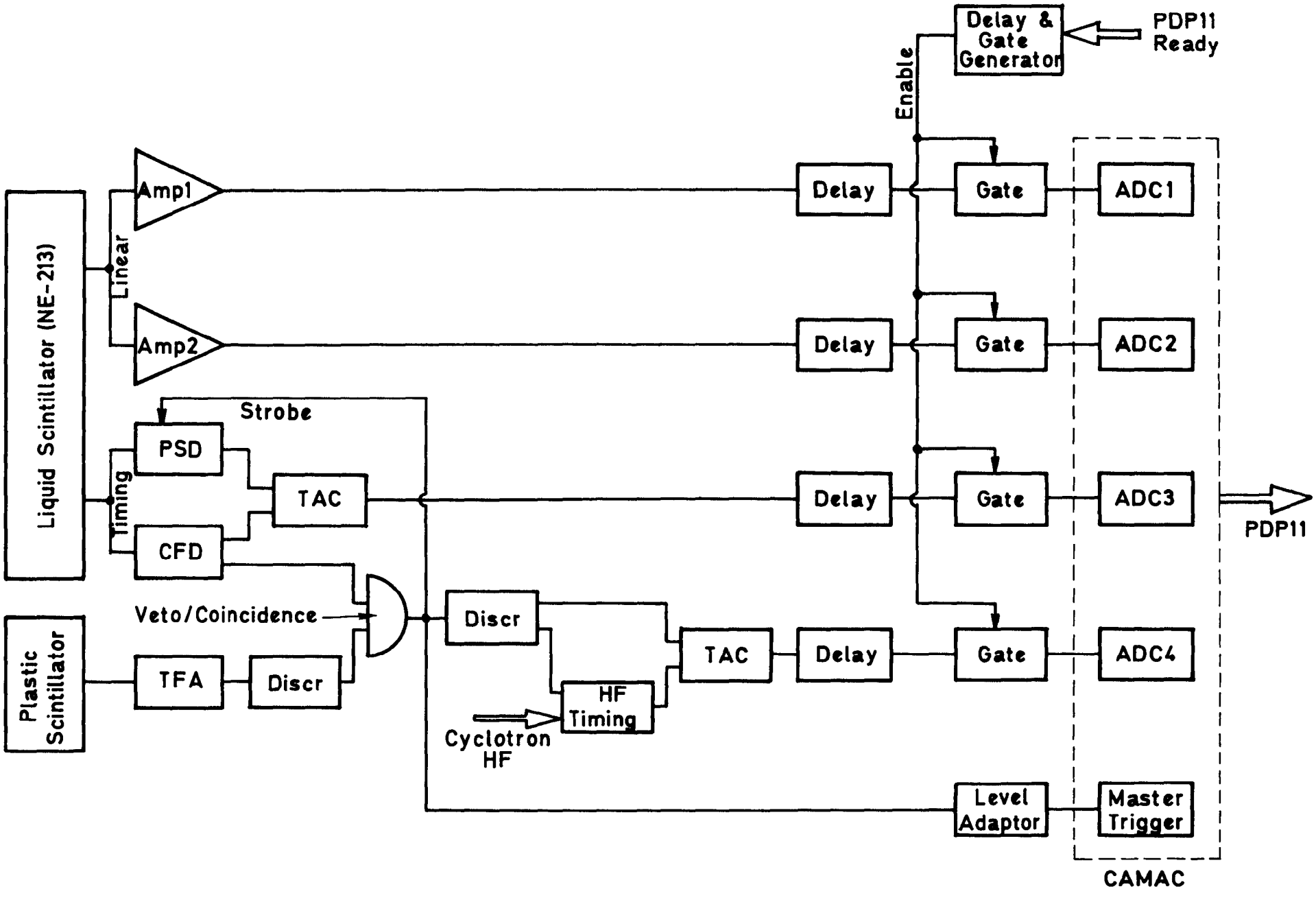


Figure 2 - Simplified circuit diagram of the electronics used in the time-of-flight experiments

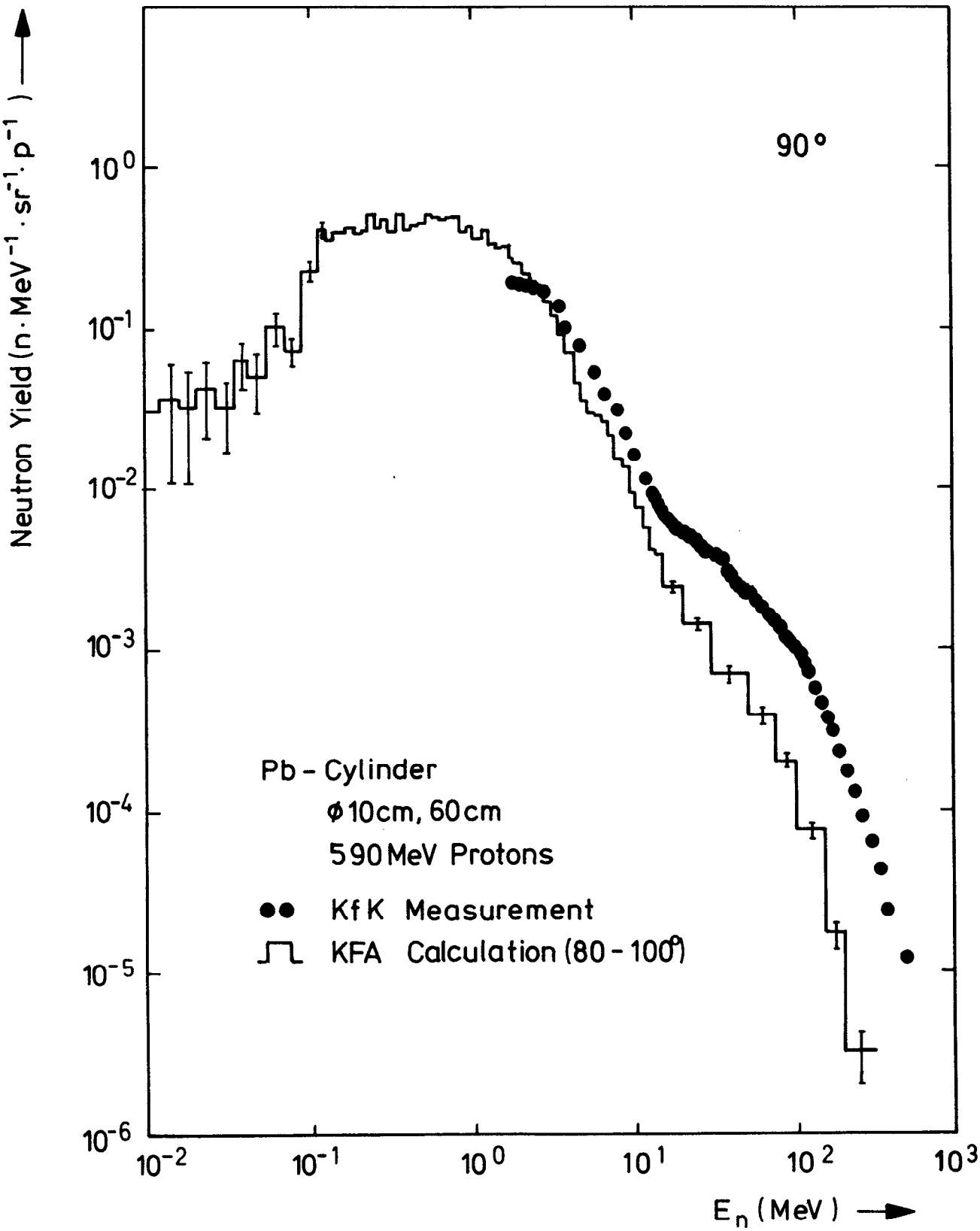


Figure 3 - Measured and calculated neutron spectra from a thick lead target at $90^{o}$ for an incident proton energy of 590 MeV

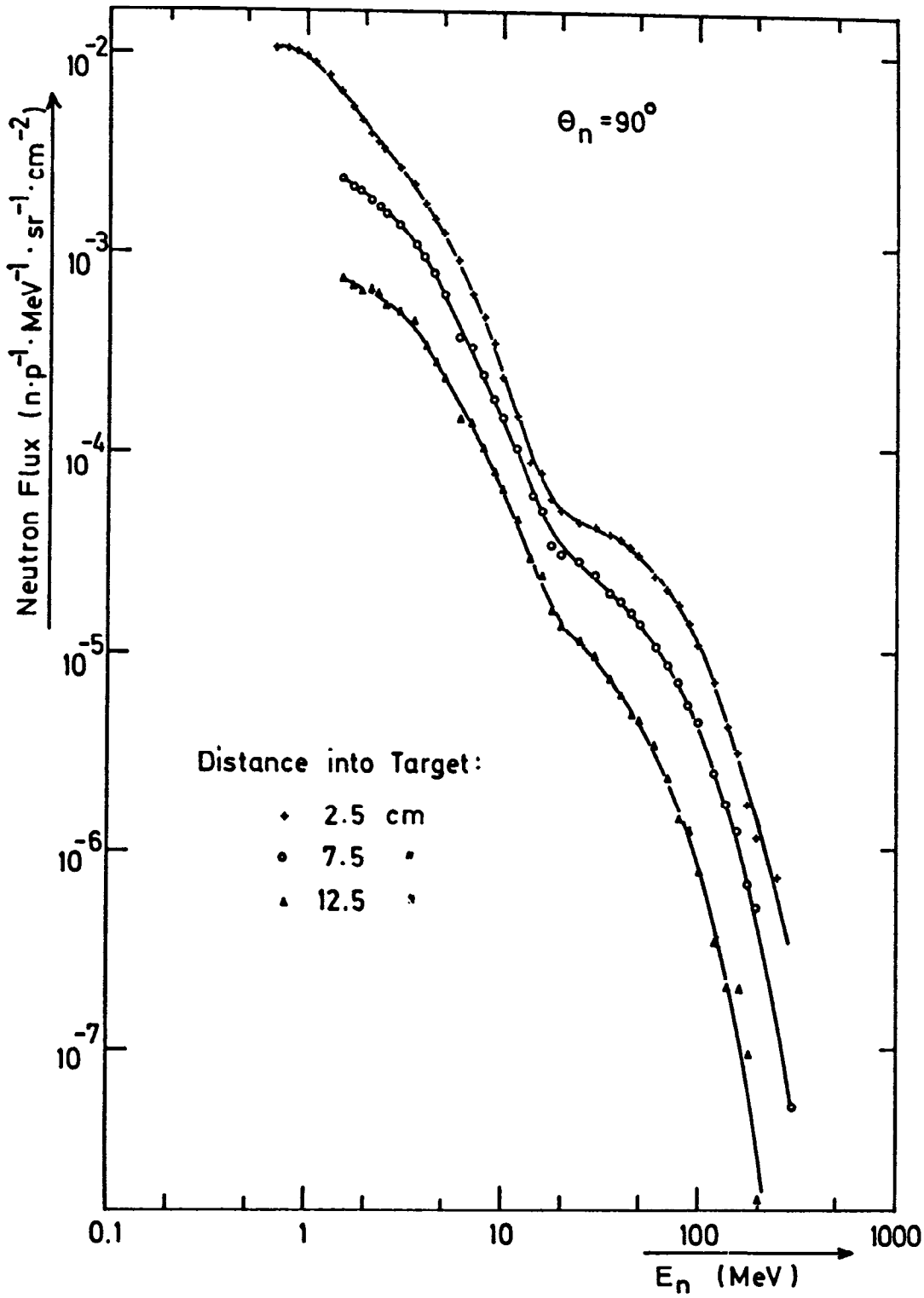


Figure 4 - Differential spectra of neutrons emitted at 90° from the first three blocks of a thick, 10x10 cm, uranium target for an incident proton energy of 590 MeV. Given data refer only to neutrons coming from the effective target volume

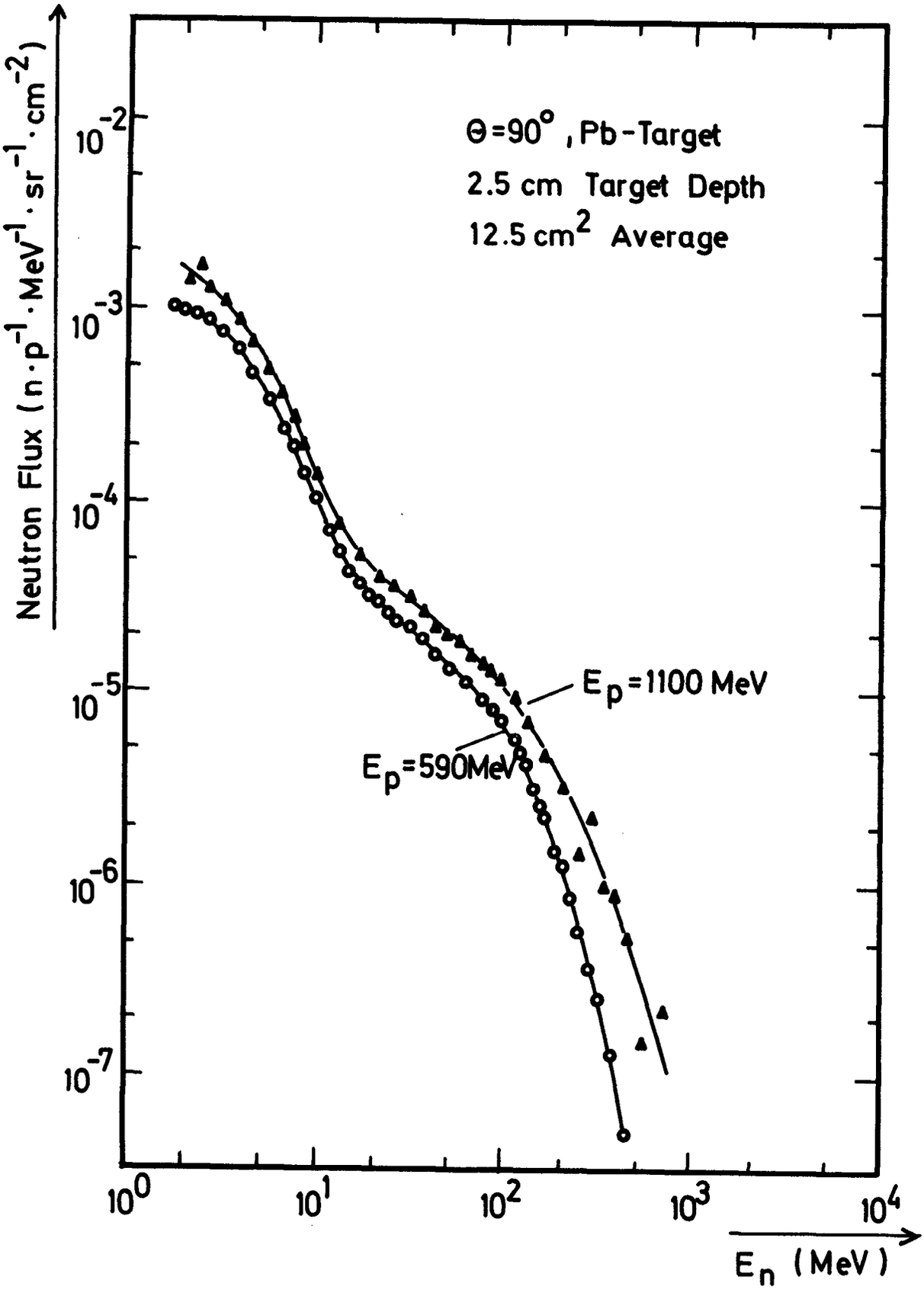


Figure 5 - Differential spectra of neutrons emitted from the first 5 cm block of a thick, 10 cm diam, lead target for incident protons of 590 and 1100 MeV. Given data refer only to neutrons coming from the effective target volume

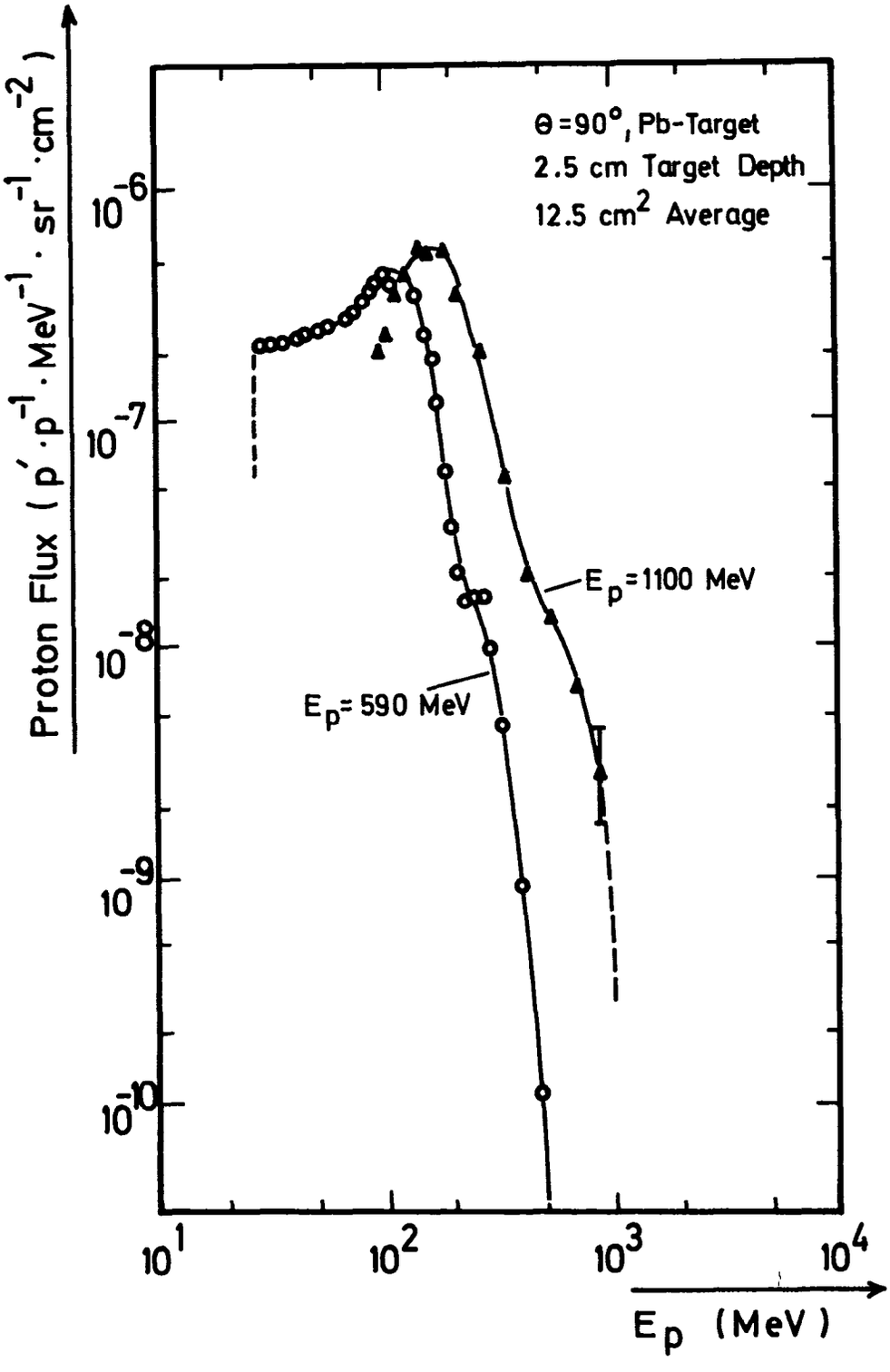


Figure 6 - Differntial spectra of protons emitted from the first 5 cm block of a thick, 10 cm diam, lead target for incident protons of 590 and 1100 MeV. Given data refer only to protons coming from the effective target volume

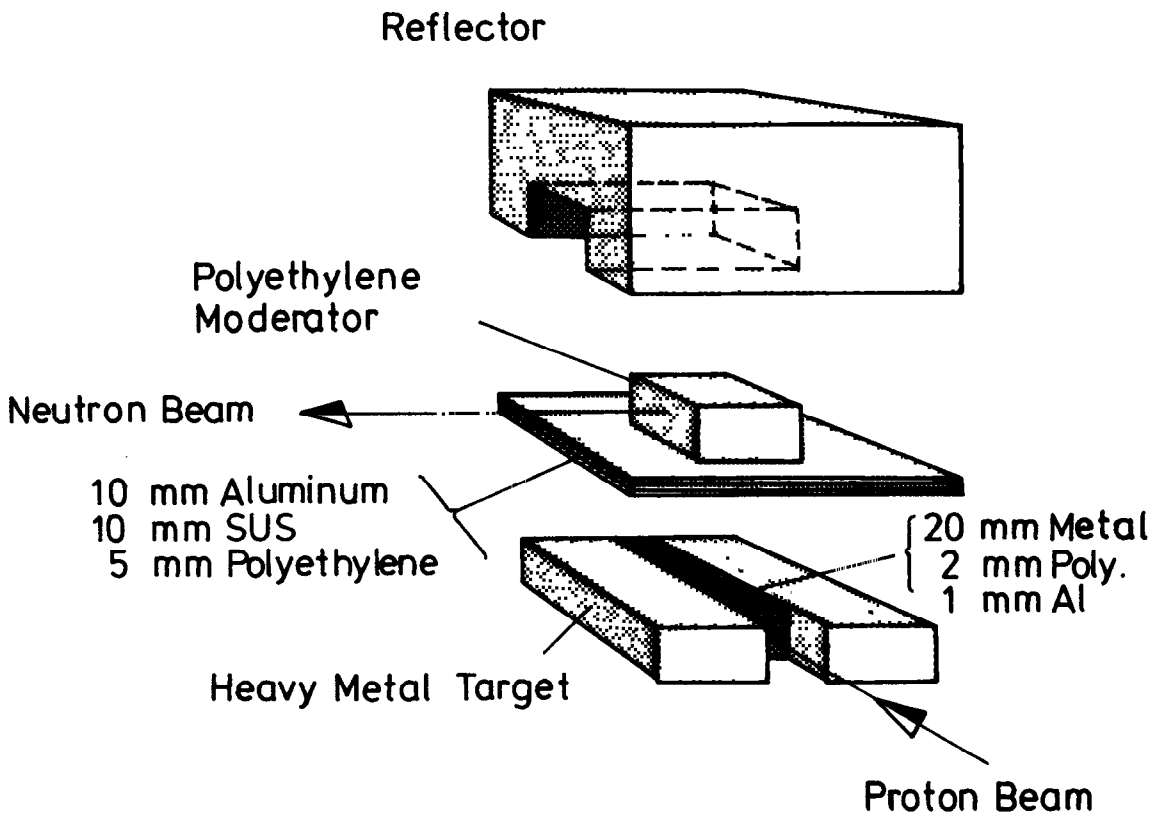


Figure 7 - Geometric arrangement of the target configurations (disassembled) studied at the SATURNE accelerator

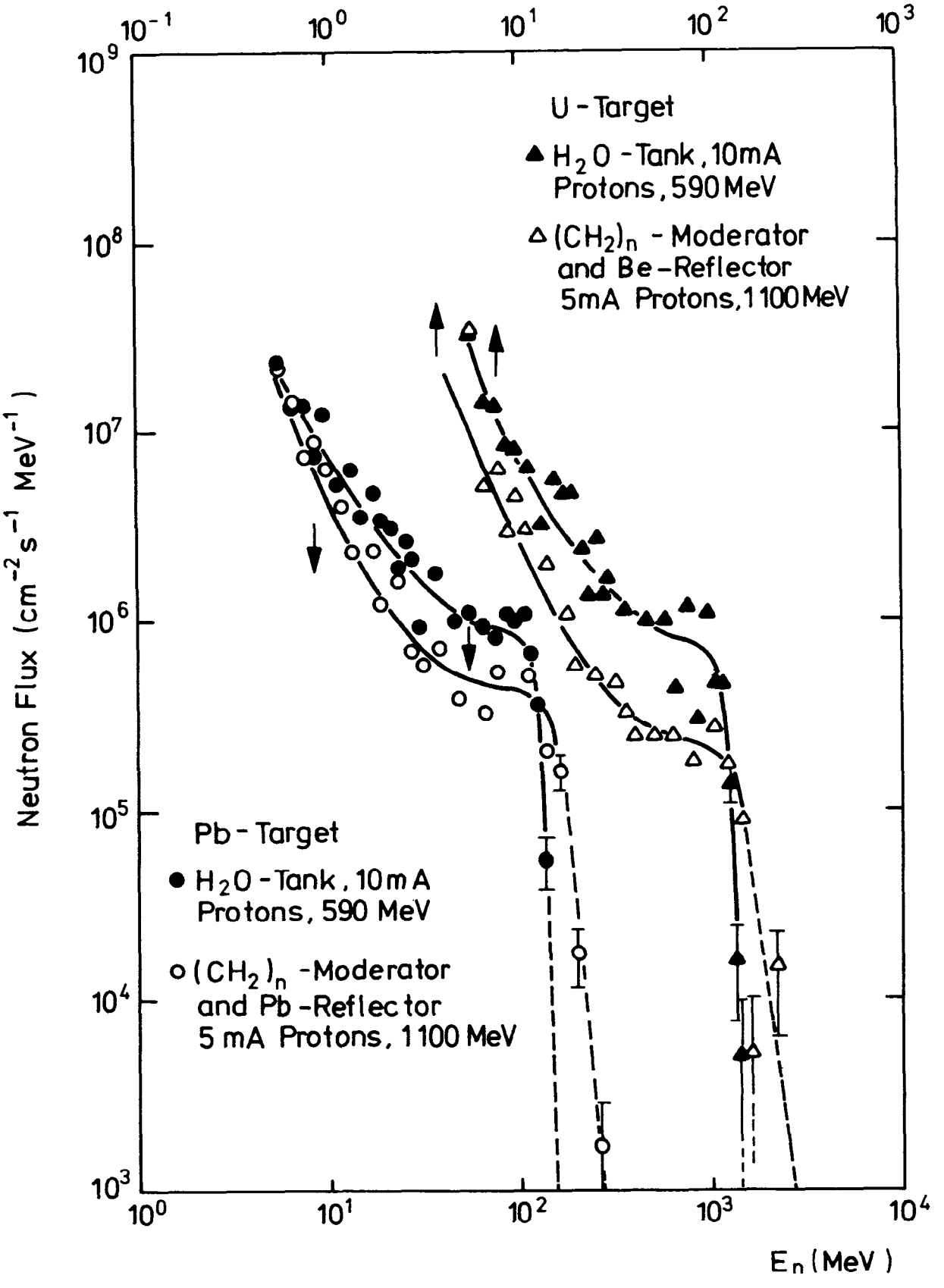


Figure 8 - High energy neutron spectra from moderated sources for several target configurations bombarded by 590 and 1100 MeV protons

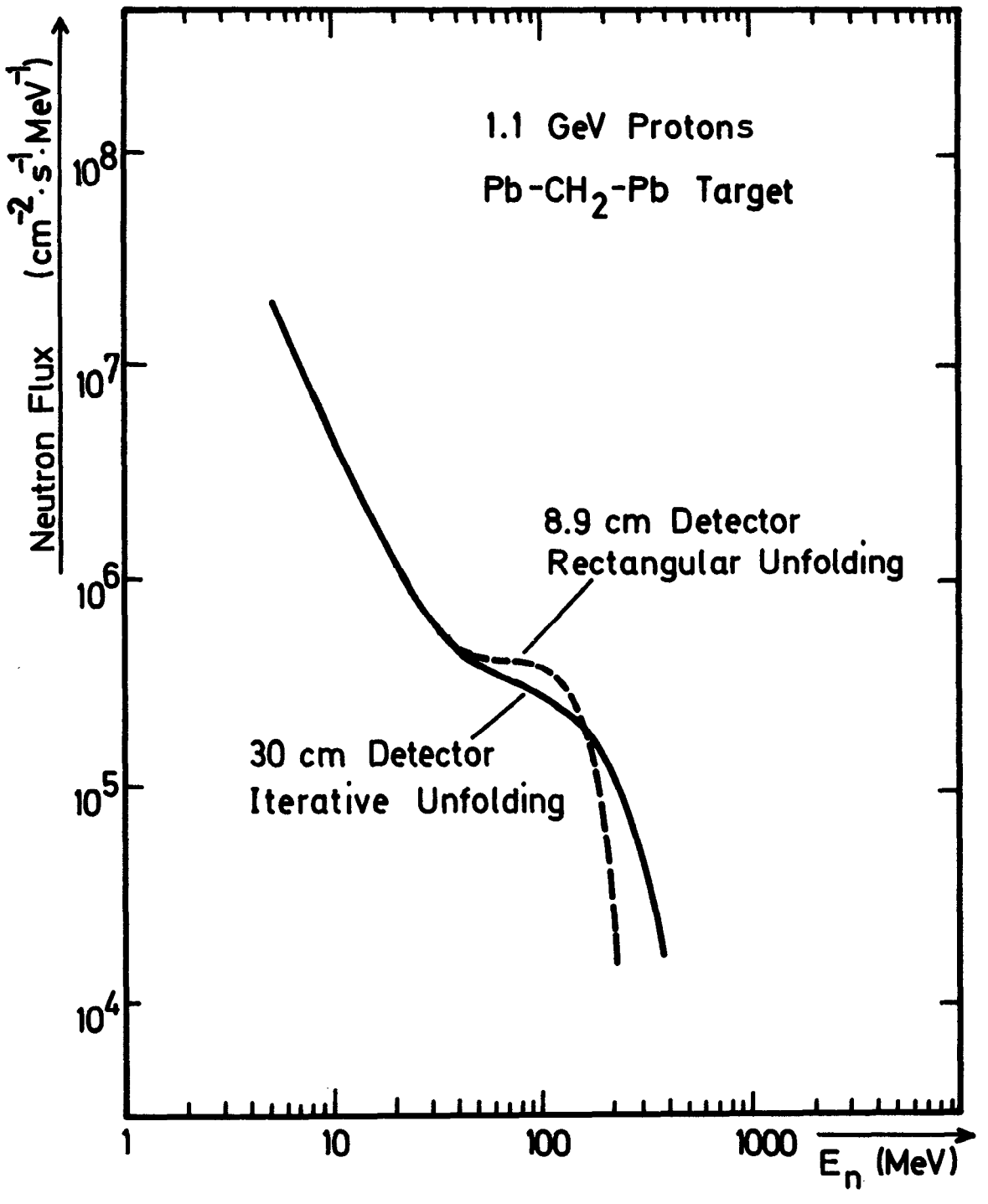


Figure 9 - Comparison of a spectrum measurement with a commercial, 8.9 cm long, liquid scintillator and rectangular unfolding and with an improved, 30 cm long, detector and iterative spectrum unfolding

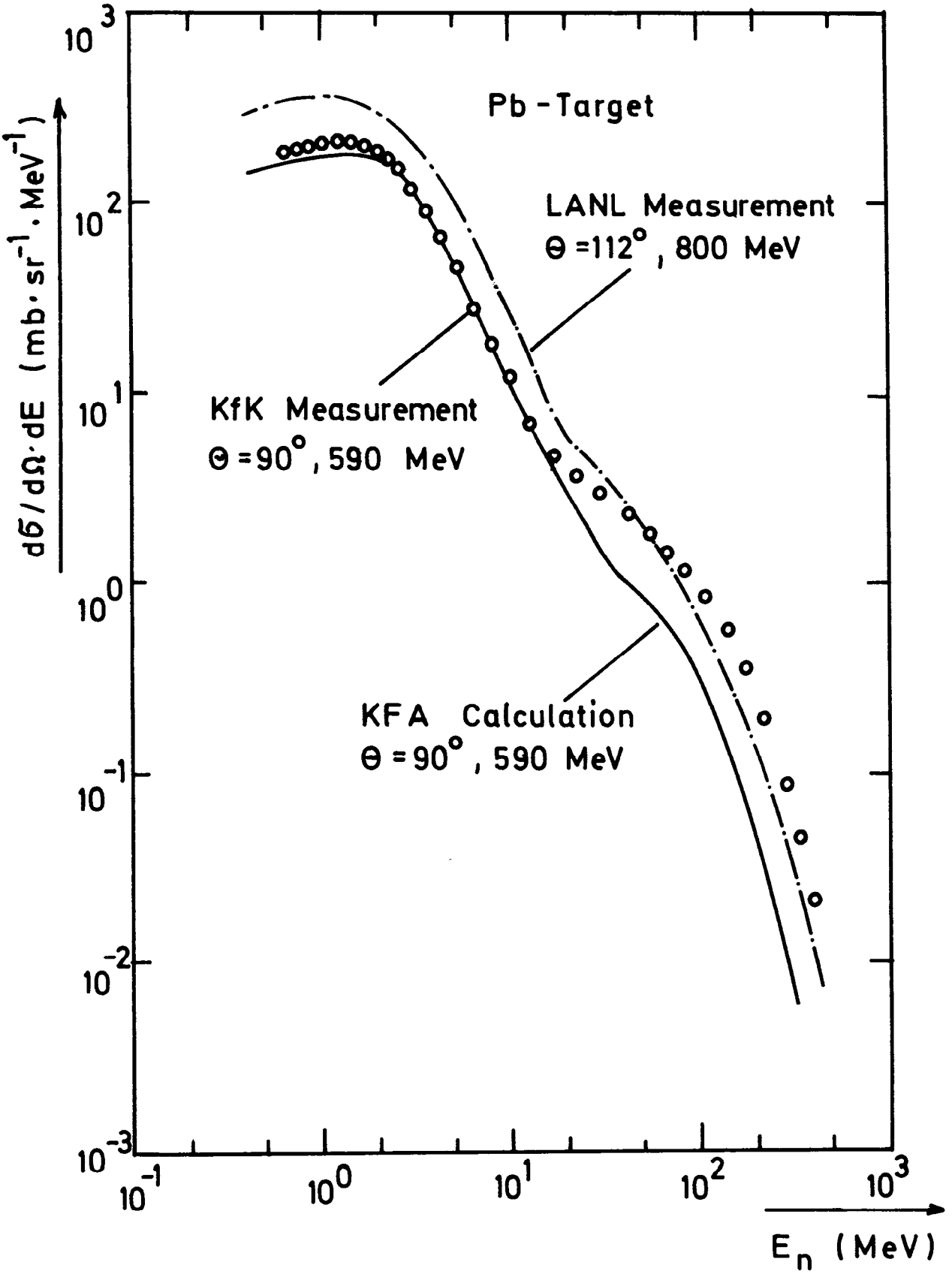


Figure 10 - Measured and calculated neutron production cross sections of lead for 590 and 800 MeV protons. The 800 MeV production cross section was taken from ref. 10

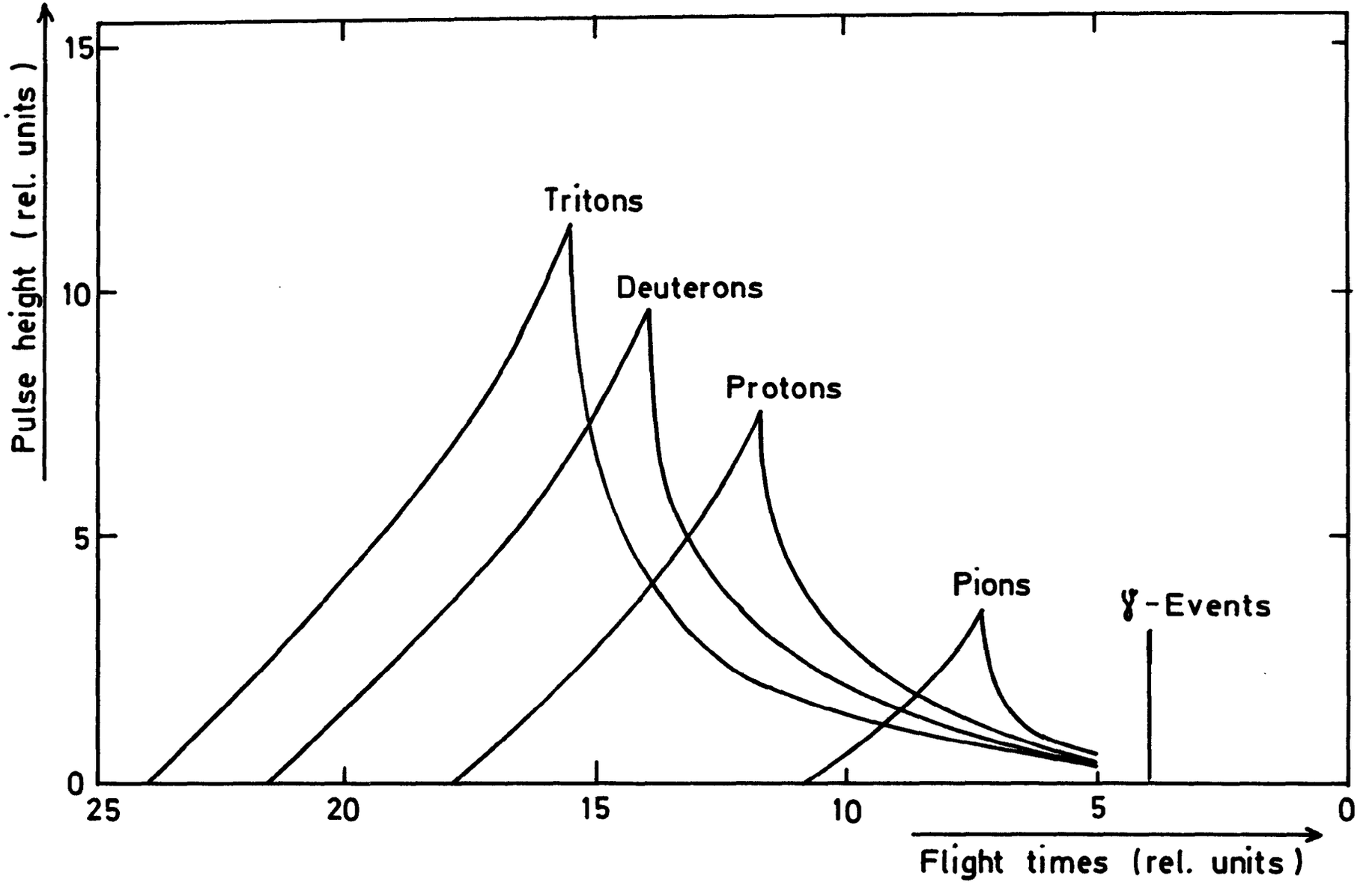


Figure 11 - Calculated relationship between energy deposition and time-of-flight for various light charged-particles. The given relationship applies for a thin detector (see text)

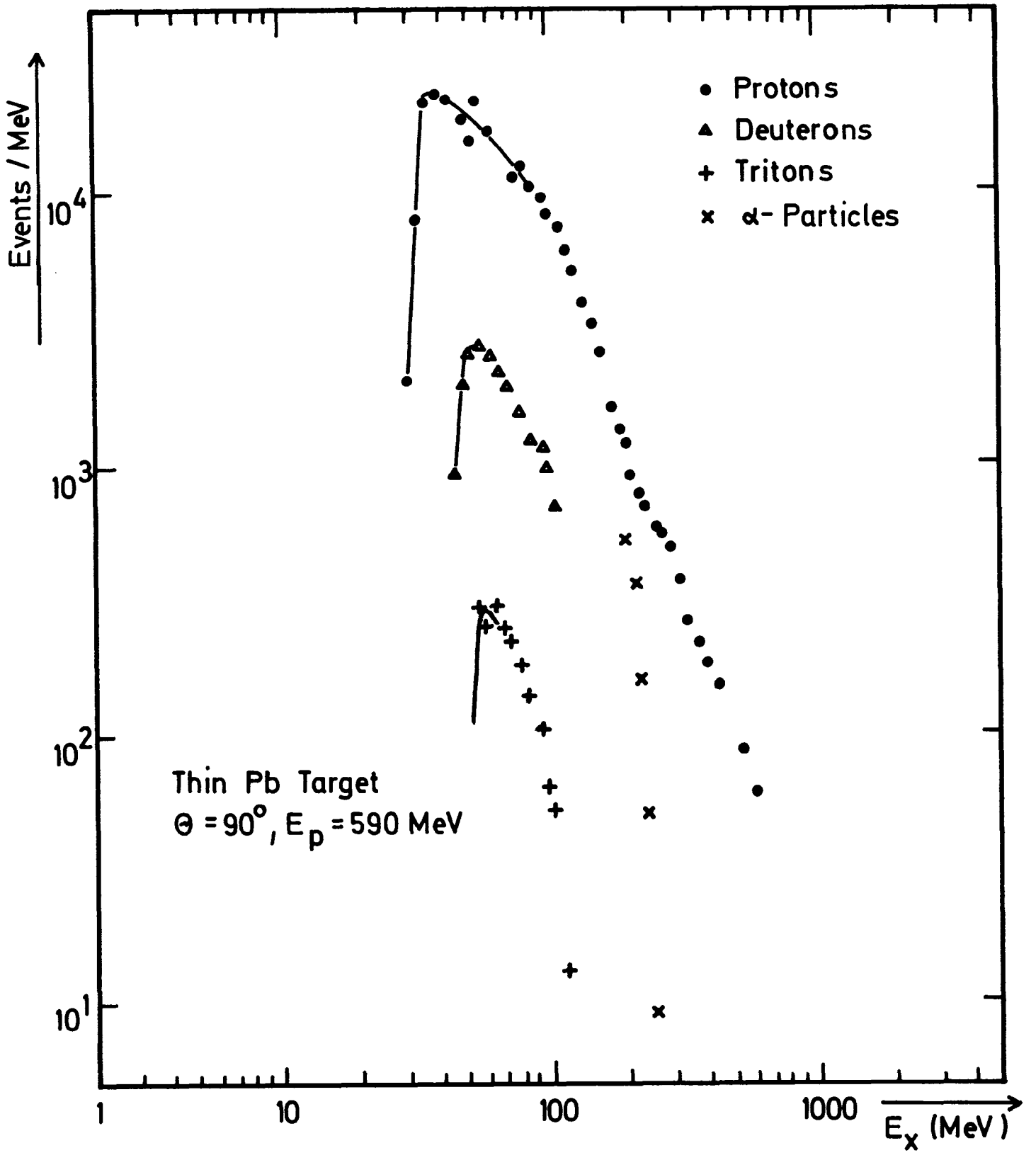


Figure 12 - Charged-particle spectra obtained at $90^{\circ}$ from a 5.6 gr/cm$^2$ lead target bombarded by 590 MeV protons. Absolute spectra from thin targets are presented in a workshop contribution of this conference (11)

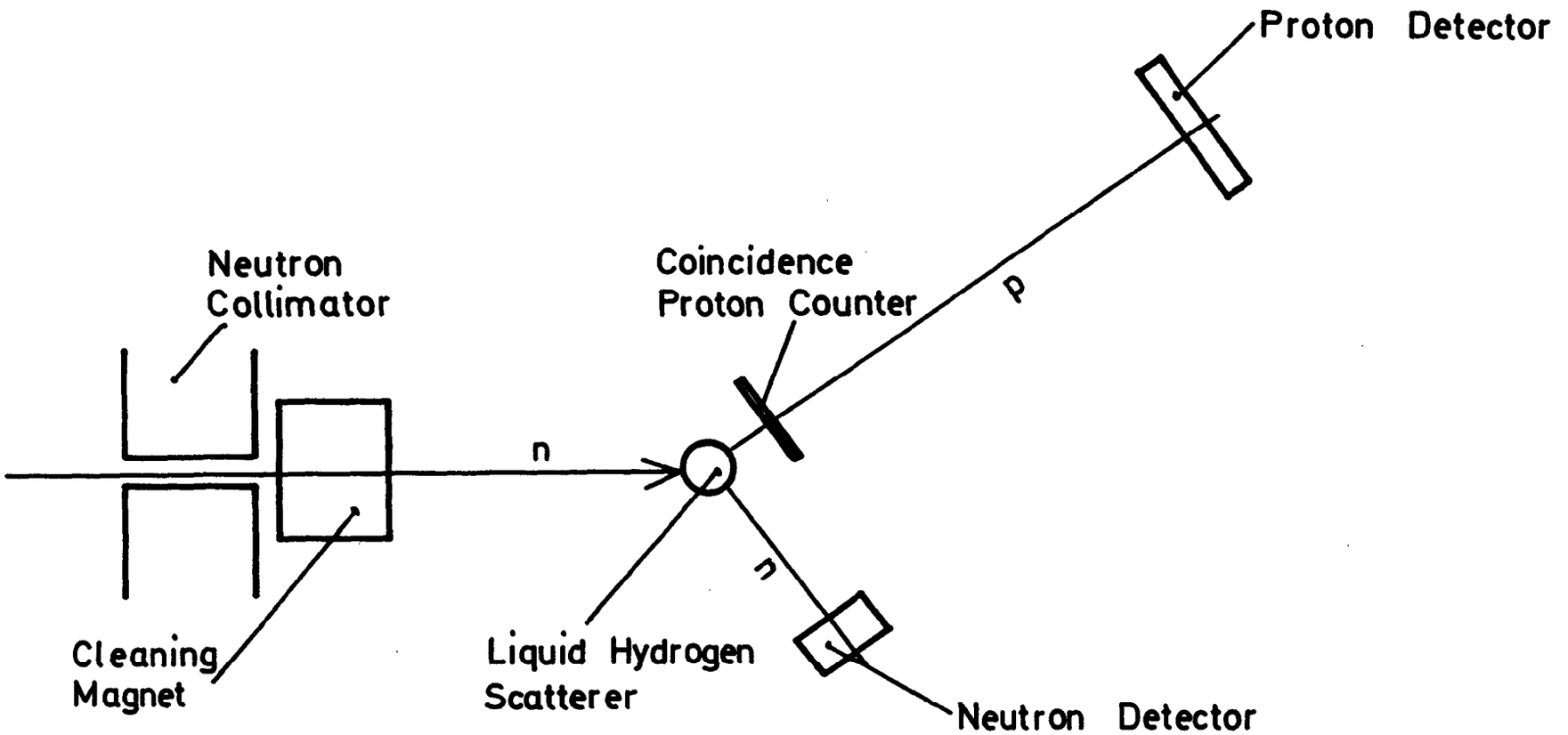


Figure 13 - Schematic drawing of the experimental arrangement used to measure neutron detection effiencies

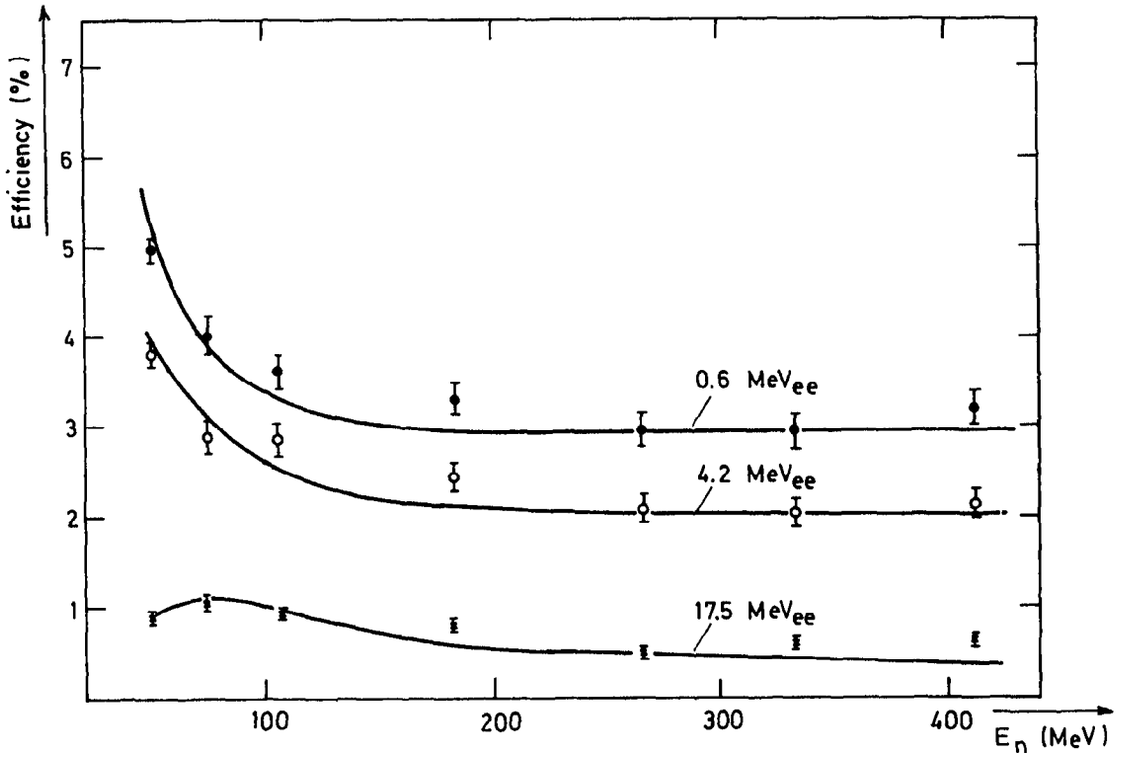


Figure 14 - Measured and calculated detection efficiencies for a 4.5 cm diameter, 3 cm thick, NE 213 liquid scintillator. Measurements and calculations were performed for detector thresholds of 0.6, 4.2 and 17.5 MeV electron energy ($MeV_{ee}$)